



Article

Improvements of the MQL Cooling-Lubrication Condition by the Addition of Multilayer Graphene Platelets in Peripheral Grinding of SAE 52100 Steel

Bruno Souza Abrão¹, Mayara Fernanda Pereira¹, Leonardo Rosa Ribeiro da Silva^{1,*}, Álisson Rocha Machado^{1,2}, Rogério Valentim Gelamo³, Fábio Martinho César de Freitas⁴, Mozammel Mia⁵ and Rosemar Batista da Silva¹

¹ School of Mechanical Engineering, Federal University of Uberlândia, Av. João Naves de Ávila, 2121, Uberlândia 38408-144, MG, Brazil; brunoabrao53@gmail.com (B.S.A.); mayaraufo2011@gmail.com (M.F.P.); alisson.rocha@pucpr.br (Á.R.M.); rosemar.silva@ufu.br (R.B.d.S.)

² Mechanical Engineering Graduate Program, Pontifícia Universidade Católica do Paraná—PUC-PR, Curitiba 80215-901, PR, Brazil

³ Institute of Technological and Exact Sciences, Federal University of Triângulo Mineiro, Av. Randolfo Borges Júnior, 1400, Uberaba 38064-200, MG, Brazil; rogerio.gelamo@uftm.edu.br

⁴ Saint-Gobain Abrasivos América do Sul, St. João Zacarias, 342, Macedo, Guarulhos 07111-150, SP, Brazil; fabio.freitas@saint-gobain.com

⁵ Department of Mechanical and Production Engineering, Ahsanullah University of Science and Technology 141-142 Love Road, Tejgaon I/A, Dhaka 1208, Bangladesh; mozammel.mpe@aust.edu

* Correspondence: leorrs@ufu.br



Citation: Abrão, B.S.; Pereira, M.F.; da Silva, L.R.R.; Machado, Á.R.; Gelamo, R.V.; de Freitas, F.M.C.; Mia, M.; da Silva, R.B. Improvements of the MQL Cooling-Lubrication Condition by the Addition of Multilayer Graphene Platelets in Peripheral Grinding of SAE 52100 Steel. *Lubricants* **2021**, *9*, 79. <https://doi.org/10.3390/lubricants9080079>

Received: 5 April 2021

Accepted: 10 August 2021

Published: 16 August 2021

Publisher's Note: MDPI stays neutral with regard to jurisdictional claims in published maps and institutional affiliations.



Copyright: © 2021 by the authors. Licensee MDPI, Basel, Switzerland. This article is an open access article distributed under the terms and conditions of the Creative Commons Attribution (CC BY) license (<https://creativecommons.org/licenses/by/4.0/>).

Abstract: In most grinding processes, the use of cutting fluid is required, and research has been carried out to reduce the amount of fluid used due to costs and environmental impacts. However, such a reduction of fluid can result in thermal damage to the machined component because the amount of cutting fluid may not be sufficient to lubricate and cool the system. One way of improving the cutting fluid properties is to add micro or nanoparticles of solid lubricants. This paper aims to evaluate the performance of multilayer graphene platelets dispersed in cutting fluid and applied through the technique of minimum quantity of lubrication (MQL) during the peripheral surface grinding of SAE 52100 hardened steel. In this sense, the influence of these solid particles with respect to the surface and sub-surface integrity of the machined components was analyzed, performing the roughness and microhardness measurement and analyzing the ground surfaces. The results showed that the cooling-lubrication conditions employing graphene could obtain smaller roughness values and decreases of microhardness in relation to the reference value and components with better surface texture compared to the conventional MQL technique without solid particles.

Keywords: grinding; multilayer graphene platelets; SAE 52100 hardened steel; minimum quantity lubrication; surface and sub-surface integrity

1. Introduction

In all machining processes, there is heat generation during material removal. In specific processes, the amount of heat generated is so significant that it can result in thermal damage to the machined component. Therefore, in most operations, cutting fluid is used to circumvent this challenge. The cutting fluids have as main functions the cooling, lubrication, and chip removal generated in the cutting zone [1].

The cooling function is associated with the system's heat removal capacity, thus reducing the amount of heat that will be directed to the workpiece. In contrast, the lubrication function reduces the friction generated during machining, reducing heat generation and power consumption. The chip removal efficiency from the grinding wheel/workpiece interface also represents a critical function since it contributes to avoiding the abrasive wheel's clogging. In addition to these functions, other requirements are expected for

the cutting fluid, such as protection against corrosion, good wettability, and recyclability, among others [2].

There are several techniques for applying the cutting fluid in the machining processes, the most employable being conventional flood cooling. In this technique, the cutting fluid is used at low pressures and high flow rates, usually above 9 L/min [3]. The purpose of using this technique is based on the fact that it uses a very high amount of cutting fluid, which increases the rate of heat dissipation.

However, the growing concern with environmental, social, and economic issues led to studying new ways of applying cutting fluids to reduce oil consumption in machining processes [4]. Unfortunately, fluid treatment is complex and often done incorrectly, negatively impacting the environment when disposal occurs. Moreover, these cutting fluids have chemical components that are harmful to human health and can cause ailments from dermatological problems to serious lung diseases. The other point, which is of most significant interest to companies, concerns the costs related to the cutting fluid, not only of purchasing, but also of maintenance and storage, among others, and according to Sanchez et al. [5] these costs can reach up to 18% of the price of a manufactured component.

One method that has emerged as an alternative to the conventional technique is the minimum quantity of lubrication (MQL). In the MQL technique, the cutting fluid is used at low flow rates, usually less than 250 mL/h, where the fluid droplets are propelled to the cutting zone by compressed air [6]. Despite presenting a significant reduction in the cutting fluid consumption (the MQL technique presents 0.1% of the flow rate found for the conventional technique), some researchers have indicated some limitations of the MQL technique related to the cooling and clogging of the grinding wheel. Due to a small amount of cutting fluid, there is low efficiency in removing the heat generated at the grinding wheel/workpiece interface, with the fluid forming a sludge with the tiny chips formed in the process, increasing the possibility of clogging the wheel. Hadad et al. [7] investigated the surface temperatures developed during grinding of 100Cr6 (SAE 52100) hardened steel with aluminum oxide and CBN wheels in different cooling–lubrication conditions (dry, MQL, and conventional). They observed that the MQL technique still has limitations in relation to the conventional cutting fluid application technique. One of the limitations is related to the fact that the MQL technique employs a much smaller amount of fluid than that used by the conventional condition, resulting in less removal of heat from the cutting zone and, consequently, and higher grinding temperatures. Bianchi et al. [8] points out that the low chip removal capacity of the cutting zone provided by the MQL cooling–lubrication conditions contributes to the occurrence of the clogging of the grinding wheel; that is, chips lodge with cutting fluid in the grinding wheel pores, which adversely affects the finish of the ground components.

Similar behavior of the low efficiency of the MQL technique in terms of heat removal from the cutting zone was observed in a study developed by Hadad and Sadeghi [9]. Hadad and Sharbati [10] performed grinding tests with an aluminum oxide grinding wheel on st37 carbon steel (DIN 17100) and different cooling delivery techniques (conventional and MQL) and observed that tests with the conventional method resulted in a reduction of the clogging phenomenon on the grinding wheel compared to the MQL technique due to the more significant amount of cutting fluid used in the process, thus providing improved chip removal from the system and, consequently, from the grinding wheel. In addition, the authors reported that the temperatures developed during the process influence this behavior, where lower temperatures are found in tests with the conventional technique because of its more significant heat transfer by convection.

Thus, new research lines have been developed to improve the MQL technique. One of the most promising is adding solid particles to the cutting fluid. The dispersion of solid particles to the fluid, which can be Al₂O₃, MoS₂, graphene, carbon nanotubes, etc., may enhance the lubricating and cooling properties of the fluids. Additionally, these solid particles act as solid lubricants at the grinding wheel/workpiece interface, improving the tribological conditions of cutting and, consequently, providing greater machining

efficiency [11–13]. It is noteworthy that one of the main problems of the MQL technique is the clogging of the grinding wheel, and some research shows that the addition of solid particles to the cutting fluid contributed to the reduction of this possibility, thus indicating another improvement of the MQL technique provided by the dispersion of lubricant solids to the fluid. According to Wojtewicz et al. [14], the dispersion of solid particles into the cutting fluid improves the tribological conditions of machining, and the authors emphasize that this behavior reduces the possibility of the occurrence of sticking of the grinding wheel.

Silva et al. [15] performed peripheral surface grinding with an aluminum oxide grinding wheel of VP 100 steel with graphene platelets (6 mg/mL concentration) added to the vegetable-based cutting fluid applied at a flow rate of 130 mL/h and comparative tests with the conventional technique. The authors reported that surface roughness was more uniform after machining with the graphene-containing cutting fluid, and, in relation to the microhardness for both cooling–lubrication conditions, microstructural changes were observed in the workpiece, and they were accentuated with cutting fluid without graphene. Chu et al. [16] evaluated graphene platelet addition at different concentrations (0.05%, 0.10%, and 0.15% by weight) in a canola-based cutting fluid in micro-machining processes. The authors reported that all concentrations investigated improved the cooling fluid's cooling and lubricating properties.

In Inconel 718 grinding tests using different cooling–lubrication conditions, Pavan et al. [17] observed that the dispersion of graphene nanoplatelets to the cutting fluid resulted in decreased cutting efforts, roughness, and temperature values, in addition to causing the generation of components with better surface texture, compared to the fluid without the addition of these solid particles. The authors justified the results because graphene increases the thermal conductivity and viscosity of the cutting fluid, promoting better lubrication and cooling.

In a recent study developed by Oliveira et al. [18], grinding tests of the Inconel 718 alloy were carried out, and the results obtained indicated that the addition of multilayer graphene platelets was beneficial because it resulted in lower values of roughness and power, better surface texture, and less variation in microhardness. In addition, the dispersion of the multilayer graphene platelets improved the cutting fluid properties and, consequently, resulted in greater lubrication and cooling of the cutting zone. In this way, the surface and sub-surface integrity of the grinding components is guaranteed.

Li et al. [19] studied the influence of graphene dispersion on the cutting fluid in terms of surface integrity (roughness and texture), temperature, and cutting forces during grinding tests on the TC4 titanium alloy. The results indicated that the addition of graphene to the cutting fluid contributed to reducing cutting efforts, temperature, Ra roughness values, and generation of a better surface texture. This behavior was found due to improved cutting fluid properties provided by graphene dispersion. Ibrahim et al. [20] also observed the benefit of adding graphene to the cutting fluid during grinding tests on the Ti-6Al-4V titanium alloy. Again, the results indicated a reduction in cutting efforts and roughness values, and improved surface texture.

To the best of the authors' knowledge, no work has been found in the literature at the time of submission of this manuscript that covers a combination of several cutting and cooling–lubrication conditions, including graphene, in grinding of SAE 52100 hardened steel, as well as an accurate characterization of cutting fluids (thermal conductivity, kinematic and dynamic viscosities). In this sense, the present work aims at evaluating the influence of graphene platelets dispersed in the cutting fluid on surface and sub-surface integrities of SAE 52100 hardened steel. Furthermore, a combination of grinding atmospheres and several cutting parameters in grinding material of great use in the industry but very susceptible to thermal damages was tested. Finally, the results obtained may contribute to the future implementation of these particles on an industrial scale.

2. Experimental Procedures

The experimental tests were performed on a semi-automatic peripheral surface grinding machine, model P36, manufactured by Mello, São Paulo, Brazil, with 3 horsepower and a rotation speed of 2400 rpm, using an aluminum oxide grinding wheel with mesh 46. The grinding machine employed has a magnetic workbench on which the precision vise containing the workpiece was positioned, as shown in Figure 1.

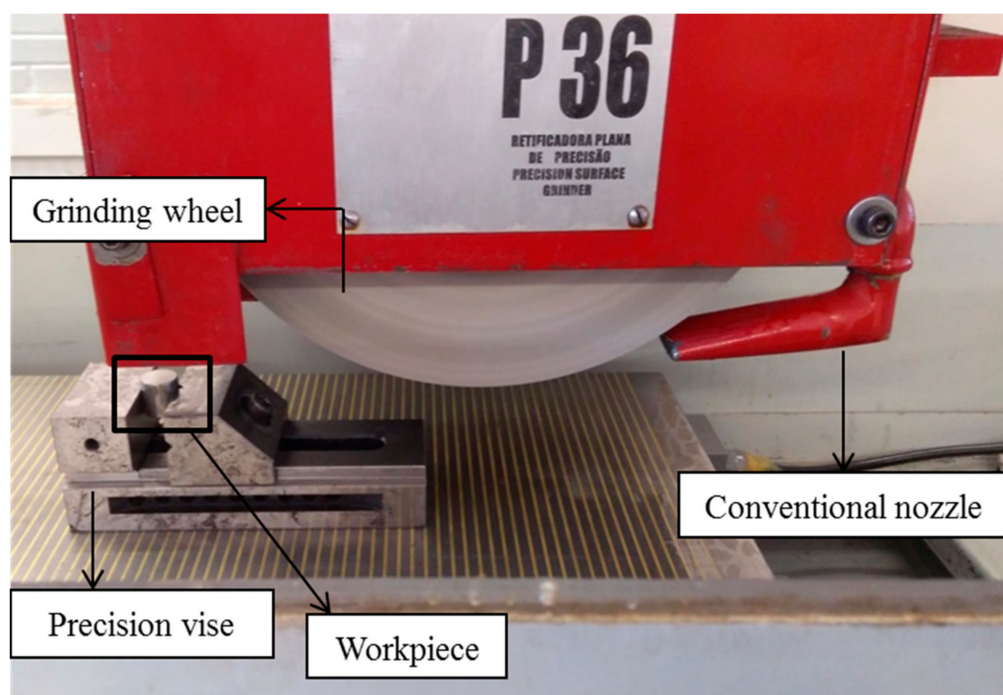


Figure 1. Representation of the components of the grinding process.

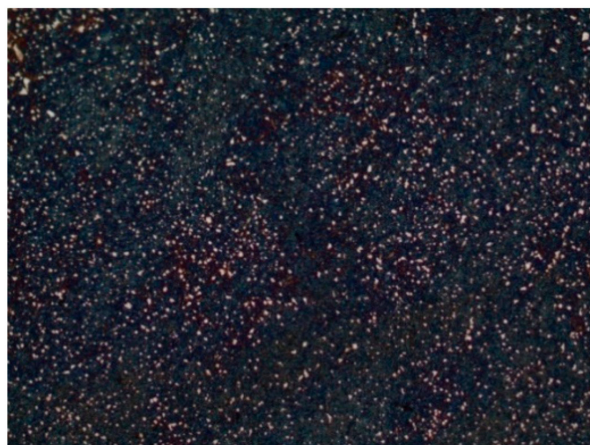
The workpiece materials were small cylinders of SAE 52100 hardened steel (60 ± 2) HRC, widely used in bearings, 16 mm in diameter and 18 mm in height. The chemical composition of this steel (wt %) and the experimental tests' parameters are shown in Tables 1 and 2, respectively. In contrast, in Figure 2, the SAE 52100 hardened steel microstructure is presented, composed of tempered martensite and retained austenite. As shown in Figure 2, the white dots present in the microstructure of SAE 52100 steel represent the carbides that compose this material. The selection of the cutting parameters occurred taking into account the limitations of the machine tool, as well as other grinding research that was carried out on a machine tool similar to that used in the experimental tests of this current work, the primary references being the studies developed by Paiva et al. [21], Guimarães et al. [22], and Hübner et al. [23].

Table 1. Chemical composition of SAE 52100 hardened steel obtained by an energy dispersive system (EDS).

Element	(wt %)
Carbon	1.03
Silicon	0.207
Sulfur	0.042
Chrome	1.526
Manganese	0.120
Iron	97.074

Table 2. Grinding conditions.

Grinding Mode	Peripheral Surface Grinding
Grinding wheel (manufactured by Norton—Saint Gobain Abrasives)	Al ₂ O ₃ : AA46K6V ($d_s = 303$ mm)
Grinding machine	Semi-automatic peripheral surface grinding P36
Cutting speed (V_s) (m/s)	37
Work speed (V_w) (m/min)	3 and 7
Radial depth of cut (a_e) (μ m)	10 and 30
Environments	Conventional, MQL, and MQL + Graphene
Conventional coolant oil technique	Water-miscible VASCO 7000 (ester–oil based) with dilution in the proportion 1:19
Conventional coolant supply flow rate (L/min)	9
MQL fluid grinding	Pure oil VASCO 7000
MQL flow rate (mL/h)	Pure oil VASCO 7000 with multilayer graphene platelets (0.050% wt)
MQL air pressure (MPa)	150
Workpiece material	0.3
Dressing operation	SAE 52100 hardened steel with 62 HRC (with 16 mm diameter and 18 mm height)
Width of dresser's performance (b_d) (mm)	Point diamond dresser
Overlap ratio (U_d)	0.3175
	5

**Figure 2.** SAE 52100 hardened steel microstructure.

Due to the constant rotation speed of the machine tool (2400 rpm), and considering the external diameter of the grinding wheel, the cutting speed was kept constant and equal to 37 m/s. Previous tests were carried out regarding selecting the workspeed values and took the grinding machine's operational range from 1 to 10 m/min. Thus, the values of workspeed of 3 and 7 m/min were those more representatives for detecting variation in surface roughness values, among other variables. Guimarães et al. [22] carried out experimental work on grinding of a mold and die steel grade (44.5 HRC) with two different grinding wheel materials (designations AA60K6V and 39C60KVK) and tested different radial depth of cut values (20, 40, and 60 μ m) and workspeed values up to 10 m/min. They found that these values were suitable to detect variations in surface roughness, microhardness below the machined surface, and residual stresses.

It is noteworthy that the main limitations found in carrying out this study are mainly related to the grinding machine, that is, in semi-automatic mode with a constant rotation speed of 2400 rpm (which hinders the use of superabrasive grinding wheels to compare the performance of grinding process with conventional abrasive grinding wheels), and also the difficulty in analyzing grinding wheel wear.

To perform the experimental tests with the MQL technique, a nozzle was developed, with one inlet for the cutting fluid and another for the compressed air. Both the nozzles of the conventional technique and the MQL were positioned at the same distance from the center of the grinding machine's main shaft (95 mm). Therefore, this variable did not exert an influence on the grinding process. This distance of 95 mm refers to that from the tip

of the nozzle to the center axis of the grinding wheel. Previous tests with several nozzle positions were carried out, so this position was the one that provided the proper access of the cutting fluid to the cutting zone for this grinding wheel–workpiece system. The control of the oil spray flow by the compressed air jet of the MQL technique was performed using a syringe pump specially designed for this purpose (Figure 3). An Arduino board with adequate programming connected to a potentiometer was responsible for adjusting the flow rate. The selected MQL flow rate was 150 mL/h, and the compressed air pressure was 0.3 MPa. This flow rate of the MQL technique and MQL air pressure was set based on previous studies [18,21,22] carried out in the same laboratory as this current work was developed. In addition, a study produced by Abrão et al. [24] indicated that grinding with a flow rate of 150 mL/h generated the best surface quality of workpieces compared to the flow rate of 60 mL/h.

Regarding solid particles, in the case of the addition of multilayer graphene, they were produced and prepared at the Laboratory of Thin Films and Plasma Processes of the Department of Applied Physics at ICTE, Federal University of Triângulo Mineiro. Then, they were dispersed in the cutting fluid at a concentration of 0.05% by weight. The choice of this concentration was based on previous studies carried out by Paiva et al. [21] and Oliveira et al. [18] in grinding of bearing steel and nickel alloy, respectively. They used the same grinding machine, oil (Vasco 7000), and coolant delivery system. They observed that the concentration of 0.05 wt% provided the lowest roughness values, best surface finish, and slightest microhardness variations, compared to 0.025, 0.075, and 0.1 wt% concentrations. The term “multilayer graphene” was taken from other studies that evaluated similar solid particles used in this work, for instance, the work developed by Oliveira et al. [18] in the grinding of Inconel 718 alloy with an SiC grinding wheel. Additionally, according to Rouxinol et al. [25], it can be considered that isolated flakes with a thickness between 5 nm to 30 nm and with a number of layers greater than five are called multilayer graphene. Wong and Akinwande [26] highlight that graphene can serve as a basis for other carbon structures and developed a table indicating the properties of carbon allotropes, thus facilitating their distinction (Table 3).

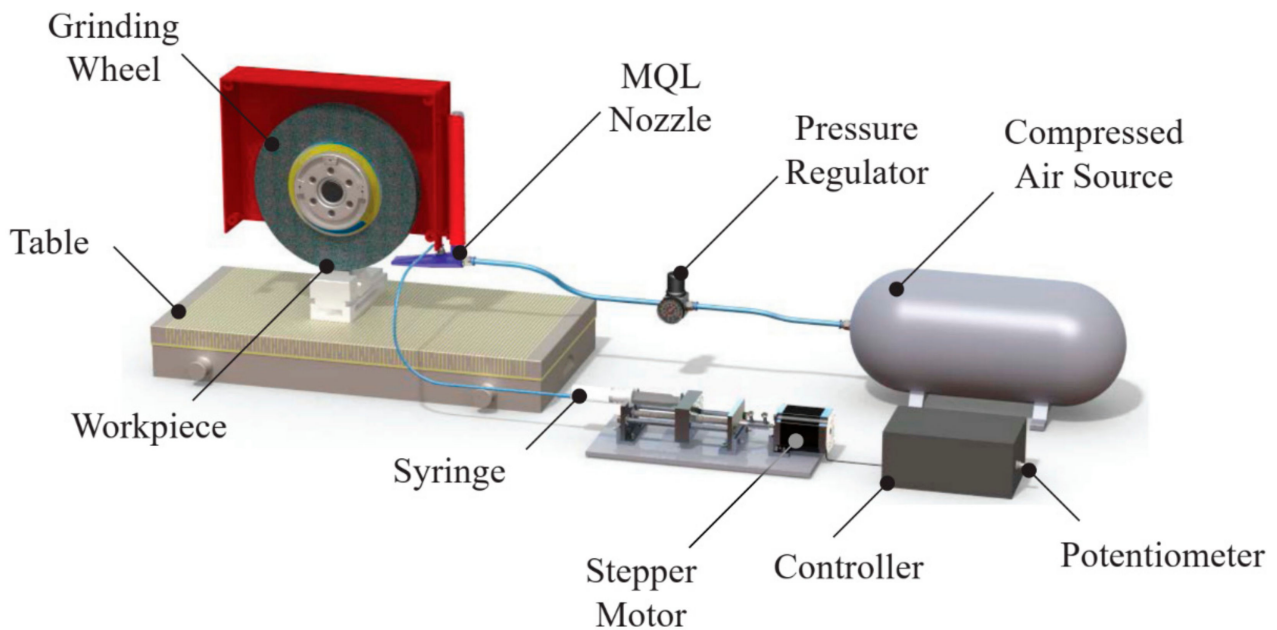


Figure 3. Schematic of the MQL coolant system delivery [27].

Table 3. Allotropes of graphene [26].

Dimension	0D	1D	2D	3D
Allotrope	C60 Buckyball	Carbon nanotubes	Graphene	Graphite
Structure	Spherical	Cylindrical	Planar	Stacked planar
Hybridization	sp ²	sp ²	sp ²	sp ²
Electronic properties	Semiconductor	Metal or semiconductor	Semi-metal	Metal

The preparation of multilayer graphene occurred through the mechanical exfoliation of graphite, the natural graphite being obtained by Nacional de Grafite Ltd.a, Itapeperica, Brazil. At the end of the preparation process, the multilayer graphene platelets had a size on the order of 1 μm to 20 μm and a thickness between 1 nm and 30 nm. The dispersion of MLG in the oil was made with the aid of a commercially available ultrasonic bath system manufactured by Soniclean Sanders Co. (Santa Rita do Sapucaí, Brazil) at a frequency of 40 kHz, with a reservoir capacity of 6 L, and at room temperature for 2 h, and time optimized for the complete dispersion of the graphene platelets in the oil herein studied. Thus, over time, some agglomeration of these solid particles could occur. Then, before carrying out each experimental test, the fluid containing multilayer graphene was placed in a vessel and taken to ultrasonic again, aiming for the complete dispersion of the multilayer graphene into the cutting fluid. Figure 4 shows the fluid (oil only) appearance before and after the dispersion of the graphene platelets.

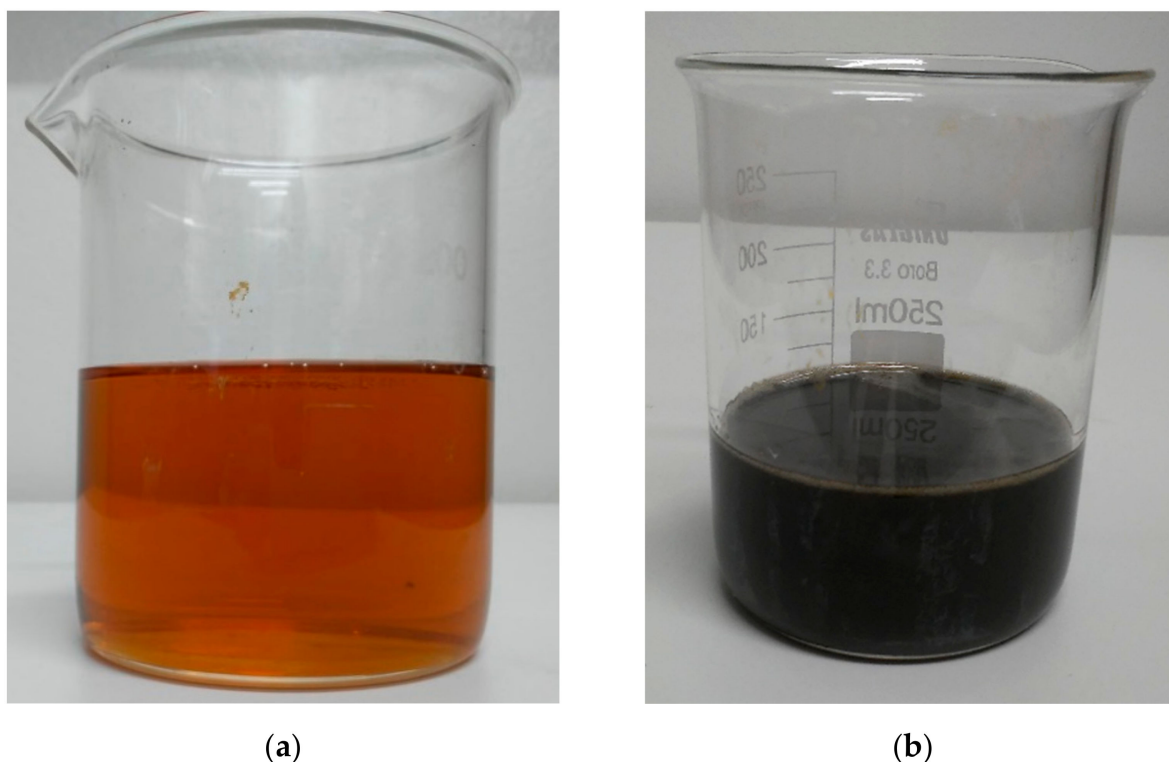
**Figure 4.** Semisynthetic cutting fluid: (a) pure; (b) with dispersed graphene platelets.

Table 4 presents some properties related to the different cooling–lubrication conditions employed.

Table 4. Properties of the cutting fluids at 25 °C employed in the experimental tests.

Cooling–Lubrication Conditions	Thermal Conductivity (W/mk)	Kinematic Viscosity (mm ² .s ⁻¹)	Dynamic Viscosity (mPa.s)	Specific Mass (g/cm ³)
Conventional (without solid particles—Emulsion at 1:19 dilution)	0.602 ± 0.001	1.084 ± 0.002	1.080 ± 0.002	0.997 ± 0.000
MQL (oil without added water and without solid particles)	0.314 ± 0.000	151.367 ± 0.148	148.542 ± 0.144	0.981 ± 0.000
MQL–Graphene (0.05% wt.)	0.321 ± 0.001	166.692 ± 2.472	163.407 ± 2.392	0.980 ± 0.001

The cutting fluids characterization procedure was carried out at the Energy, Thermal Systems and Nanotechnology Laboratory (LEST-NANO), at the Faculty of Mechanical Engineering of the Federal University of Uberlândia. The measurement of viscosity values was performed with the aid of an Anton Paar, Stabinger viscometer, model SVM 3000 (São Paulo, Brazil), with three measurements (measurement + two replicates) being performed for each fluid sample evaluated. For thermal conductivity measurement, a Linseis THB-1 conductivity meter was also present in LEST-NANO.

The influence of cutting fluid containing graphene platelets compared to the conventional technique and MQL without the addition of graphene was evaluated by measuring the surface roughness and microhardness, in addition to the analysis of ground surface images. R_a and R_z roughness parameters were measured through a portable surface roughness tester Taylor Hobson, model Surtronic S-100 (São Paulo, Brazil), with a resolution of 0.01 µm. The measurement of this parameter occurred on five regions on the machined surface, and a cut-off of 0.8 mm and a sampling length of 4 mm were employed. All measurements were performed on the faceplate, ensuring parallelism with the measuring surface under controlled temperature and humidity conditions. Furthermore, since the two surfaces of the workpiece were ground, the pieces were fixed in a precision vise to guarantee rigid support and no interference of positioning errors in the measurements.

Before the microhardness measurements, ground workpieces were sanded employing silicon carbide sandpapers with 220, 320, 600, 800, 1000, and 1200 mesh and then polished using alumina paste of 0.1 µm size (metallography technique). Although the choice of carrying out the polishing process before measuring microhardness was due to in other works on grinding, the polishing process was also used successfully before the measurement of microhardness, as in a study developed by Silva et al. [28], Moraes et al. [29], Srivastava et al. [30], Javaroni et al. [31], and Garcia et al. [32]. The microhardness was evaluated using a SHIMADZU HMV-2 series hardness tester with a Vickers penetrator (Barueri, Brazil). A load of 490.3 mN (0.05 HV) was applied for 15 s to measure this parameter. The start of measurements occurred from 30 µm below the ground surface at intervals of 30 µm (Figure 5). Three measurement cycles were performed, in different regions, in order to obtain the average microhardness values.

The ground surfaces were analyzed using a scanning electron microscope (SEM), model TM3000 (São Paulo, Brazil), equipped with an energy dispersive spectroscopy (EDS) device to verify cracks and adhered material in addition to the marks originated from the process. For this, the pieces were cleaned with the aid of a sonicator and a vessel with pure acetone to remove chips, impurities, and even cutting fluid left on the workpieces' surfaces. Before the analyzes, the samples were fixed in a miniaturized precision vise within the SEM.

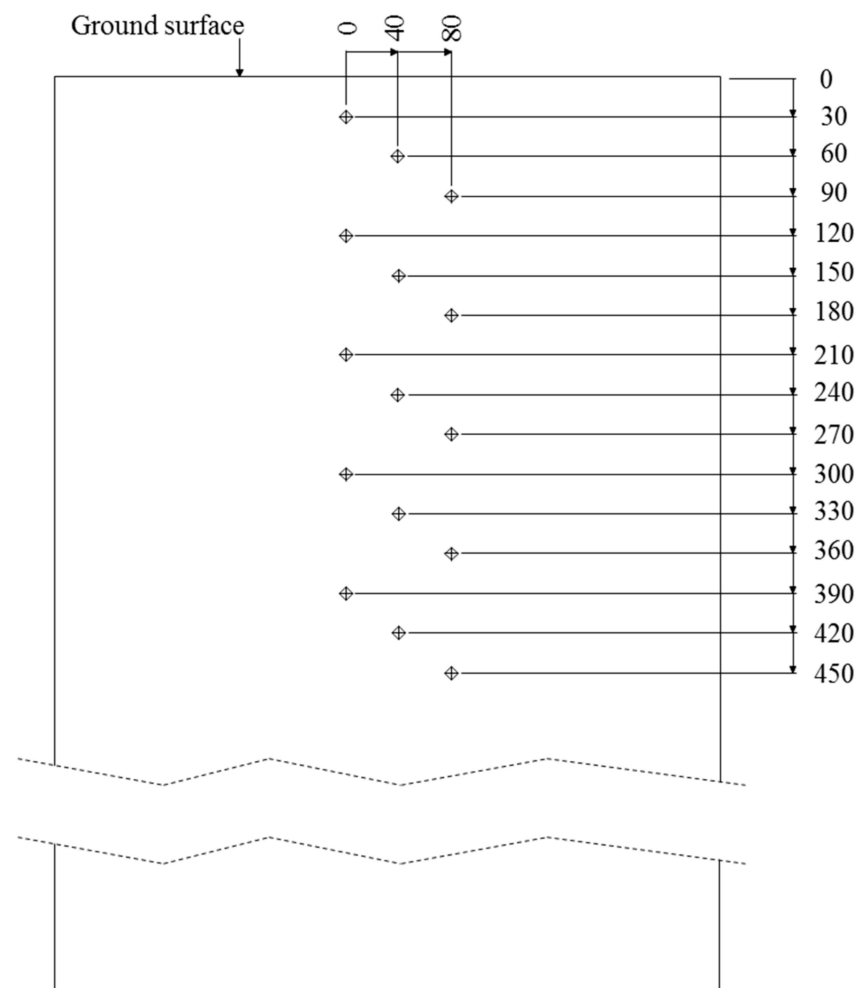


Figure 5. Measurement microhardness (μm).

3. Results and Discussion

This section presents and discusses the results of surface roughness, microhardness profiles, and the ground surfaces' images obtained after the grinding of the SAE 52100 hardened steel with a white aluminum oxide grinding wheel under various cutting conditions.

3.1. Surface Roughness

The roughness results for R_a and R_z parameters of all cooling–lubrication conditions employed are presented in Figures 6 and 7, respectively. Again, the values are grouped according to the radial depth of cut (a_e) and workspeed (V_w).

In general, R_a and R_z roughness parameters increase with the increase of the radial depth of cut (a_e), and this behavior is best visualized in the parameter R_z . Although R_a is one of the most used parameters, it does not depict flaws because it is an arithmetical mean roughness parameter. Therefore, other parameters are necessary for better characterization of the irregularities of the surface [33], such as the average pick-to-valley roughness R_z .

According to Malkin and Guo [34], the increase of the variable a_e causes increased abrasive grits acting during the process. Consequently, the contact time of these with the workpiece, and thus the portion of material removed by each abrasive becomes smaller, favoring the formation of thin and elongated chips. Therefore, there is a higher fraction of friction and scratching between the chips and the workpiece, causing the temperature rise in the cutting region, in addition to the increased roughness of the workpiece, cutting forces, and acoustic emissions.

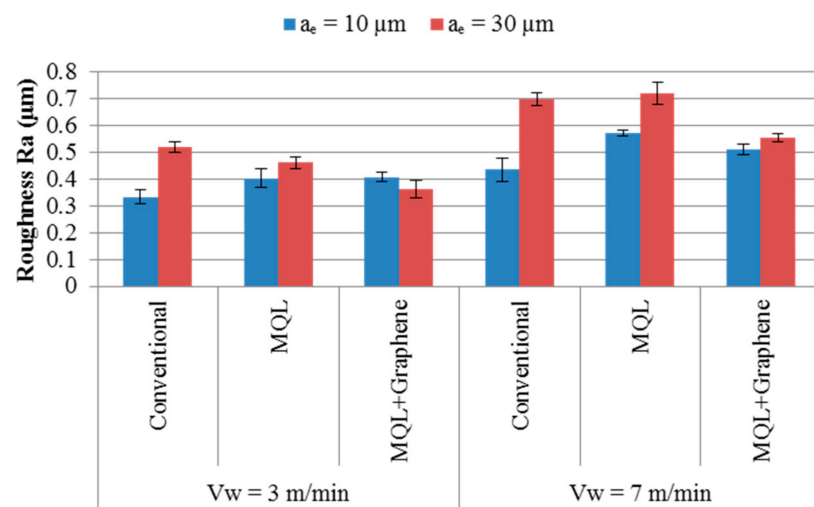


Figure 6. Roughness values, R_a , for the SAE 52100 hardened steel obtained after peripheral surface grinding in different cooling–lubrication and cutting conditions.

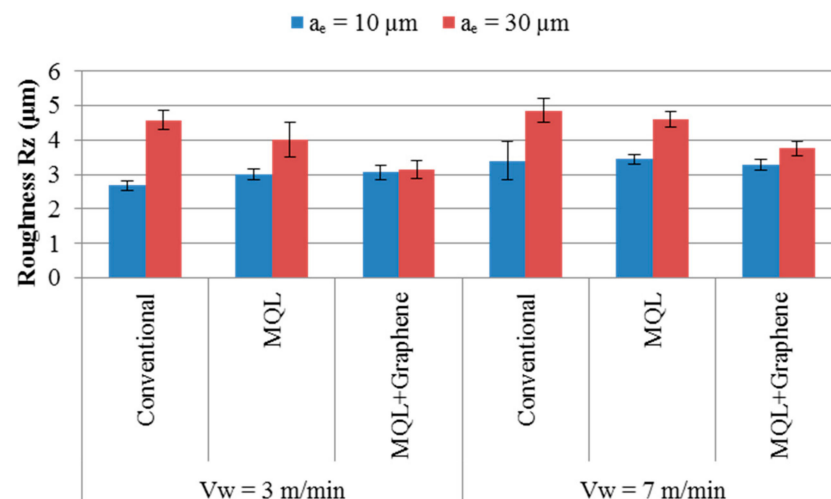


Figure 7. Roughness values, R_z , for the SAE 52100 hardened steel obtained after peripheral surface grinding in different cooling–lubrication and cutting conditions.

As can be seen from Figure 6, the tests performed with a radial depth of cut of 30 µm showed a more uniform trend compared to the use of $a_e = 10$ µm. Moreover, for the R_a parameter, in some tests the average value obtained with the employment of $a_e = 10$ µm was higher than that performed using $a_e = 30$ µm. One possible explanation concerns the machine having a certain gap in the system for selecting the radial depth of cut value, and in the case of an a_e value of 10 µm, this gap becomes more significant due to the magnitude of the variable. In this sense, the minimum cutting thickness may not be reached, thus only deforming material without actually causing the chip to be removed, negatively affecting the surface roughness. According to Lin et al. [35], the depth of the abrasive grits during the grinding process is a factor of significant influence on the morphology of the machined surfaces, that is, on the finish and, consequently, on the roughness values of the ground components. Therefore, the depth of grits plays an essential factor in chip formation during grinding. If the grit or setting depth is insufficient to generate the minimum cutting thickness, only deformation of the material occurs instead of the removal stage and consequently chip formation.

In order to measure the difference in the analyzed roughness parameters (R_a and R_z) by varying the radial depth of cut from 10 to 30 µm and the work speed from 3 to 7 m/min

and to be able to identify any trend, Tables 5 and 6 were prepared, which presents the results obtained for the different cooling–lubrication conditions.

Table 5. Influence of the radial depth of cut on the R_a and R_z roughness parameters.

Cooling–Lubrication Condition	Workspeed (m/min)	Roughness Parameter	Percentage Variation (%)
Conventional	3	R_a	55.7
		R_z	70.9
	7	R_a	60.1
		R_z	42.9
MQL	3	R_a	14.4
		R_z	34
	7	R_a	25.4
		R_z	33.7
MQL + Graphene	3	R_a	−10.8
		R_z	2.6
	7	R_a	9.0
		R_z	14.6

Table 6. Influence of the workspeed on the R_a and R_z roughness parameters.

Cooling–Lubrication Condition	Radial Depth of Cut (μm)	Roughness Parameter	Percentage Variation (%)
Conventional	10	R_a	30.54
		R_z	26.87
	30	R_a	34.23
		R_z	6.11
MQL	10	R_a	42.08
		R_z	14.67
	30	R_a	55.84
		R_z	14.43
MQL + Graphene	10	R_a	25
		R_z	7.19
	30	R_a	52.75
		R_z	19.74

As shown in Table 5, the MQL + Graphene cooling–lubrication conditions resulted in the lowest percentage variation of the values obtained. At the same time, the conventional cutting fluid application was responsible for the most remarkable variations with the increase in radial depth of cut. Regarding the influence of the workspeed variation (Table 6), similar behavior was observed for all the cutting and cooling–lubrication conditions evaluated, and for all conditions, the increase in V_w increased in R_a and R_z .

The increase of the workspeed (V_w) also caused an increase in the roughness parameters. This result is explained based on the equivalent chip thickness (h_{eq}). According to Rowe [1], the increment of this variable leads to an increase in the material thickness that is removed in an entire revolution by the grinding wheel, that is, the parameter h_{eq} ($h_{eq} = a_e \cdot \frac{V_w}{V_s}$). Thus, with an increase in the equivalent chip thickness, the tensile stress on the abrasive grits and, consequently, on the shearing forces increase, and deterioration of the workpiece’s roughness occurs. As can be seen in Figures 6 and 7, the increase in V_w

from 3 m/min to 7 m/min resulted, in general, in the increase in the R_a and R_z roughness parameters, and for the parameter R_z , this increase is better visualized through the analysis of the results obtained after the experimental tests employing the highest radial depth of cut value ($a_e = 30 \mu\text{m}$). This behavior was also demonstrated in Table 4, where for all the conditions of cutting and cooling–lubrication evaluated, it was observed that the increase in the workspeed indicated an increase in the R_a and R_z roughness parameters. The influence of the variables radial depth of cut and workspeed was evaluated by Tawakoli et al. [36]. The authors performed plunge surface grinding of 100Cr6 steel (SAE 52100) with an aluminum oxide grinding wheel under different cutting and cooling–lubrication conditions (dry, MQL, and conventional), using three values of workspeed (2.5 m/min, 5 m/min, and 10 m/min) and four radial depths of cut (5 μm , 10 μm , 15 μm , and 25 μm). It was observed that the roughness parameters evaluated (R_a and R_z) increased with the a_e and V_w , and, in general, the cooling–lubrication technique that obtained the best roughness results was MQL. Sadeghi et al. [37] also verified increased roughness (R_a) with a_e and V_w .

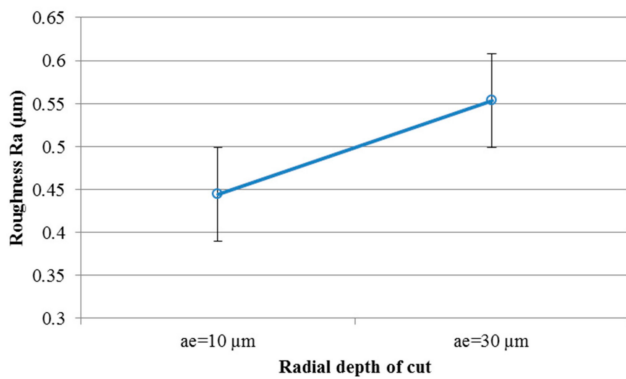
Among all the cooling–lubrication conditions employed, multilayer graphene platelets' addition to the cutting fluid contributed to the surfaces with the lowest roughness values. These particles act by reducing the friction between the grinding wheel and the workpiece, thus favoring the achievement of better-finished surfaces. Research by Gao et al. [38] investigated the tribological performance of vegetable cutting fluid containing platelets of carbon nanotubes (CNT) during friction tests simulating the grinding process, using AISI304 steel and an aluminum oxide wheel (WA80H12V). The addition of the CNT platelets contributed to the increase in the cutting fluid viscosity, resulting in a stable tribo-film and thus in the improvement of the lubricating properties of the fluid, and consequently, positively affecting some variables used to analyze the surface and sub-surface integrity of ground components, such as roughness. The study of the behavior of the efficiency of the addition of particles in cutting fluids in the grinding processes of steel with the aluminum oxide grinding wheel also occurred in a study developed by Huang et al. [12]. They tested the addition of multilayer carbon nanotubes to the cutting fluid (0.25% by weight) under different cutting and cooling–lubrication conditions. When comparing the results obtained with the condition MQL + carbon nanotubes with those obtained by the MQL condition without solid particles, the authors reported that the lower values of roughness were obtained in the carbon nanotubes' presence because these nanoparticles act in the improvement of the lubricant property of the cutting fluid. Mao et al. [39] also observed a positive influence of the addition of Al_2O_3 particles in the cutting fluid in the grinding process of the 52100 hardened steel (100Cr6), where the roughness values obtained by using the MQL + Al_2O_3 condition were comparable to those found in the tests performed using the conventional cutting fluid application technique (flooding).

Analysis of variance (ANOVA) was performed to evaluate the influence of the input variables (radial depth of cut, workspeed, and cooling–lubrication condition) and the interaction between them. Analysis of variance (ANOVA) was performed using Excel 2016 software. The p -values of these variables are presented in Table 7, where p -value < 0.05 (for statistical reliability of 95%) represents that the variable is significant for the roughness parameter, whereas p -value > 0.05 indicates that it is not significant. As shown in Table 7 through the p -value analysis, only the workspeed (V_w) significantly influenced the R_a roughness parameter. On the other hand, only the radial depth of cut significantly influenced the parameter R_z . In Figure 8, the graphs show the trend effect of the input variables on the roughness parameters of R_a and R_z . As can be observed, the increase of a_e and V_w was responsible for raising the values of R_a and R_z , while with respect to the cooling–lubrication conditions, the addition of the graphene platelets to the cutting fluid contributed to obtaining the lowest values for both roughness parameters. The increase in a_e provided an average increase in R_a of 24.53% (Figure 8a) and for the parameter R_z of 32.34% (Figure 8d), while the increase in V_w indicated an average increase of 40.21% for R_a (Figure 8b) and 13.97% for R_z (Figure 8e). In addition, among the cooling–lubrication conditions, MQL + Graphene was responsible for obtaining surfaces with lower roughness

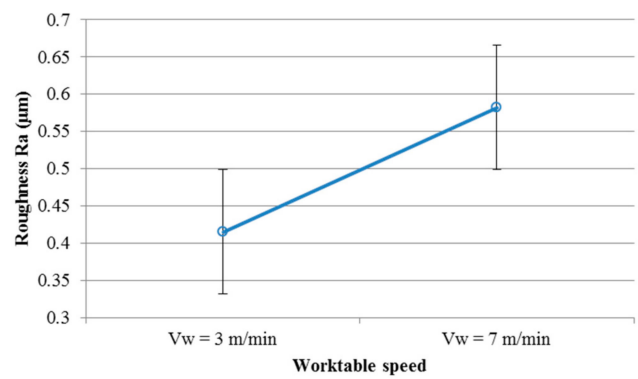
parameters (0.4595 μm for R_a (Figure 8c) and 3.31 μm for R_z (Figure 8f)) than conventional, which in general presented the more significant 0.497 μm for R_a (Figure 8c) and 3.88 μm for R_z (Figure 8f).

Table 7. Analysis of variance (ANOVA) for the roughness parameters R_a and R_z .

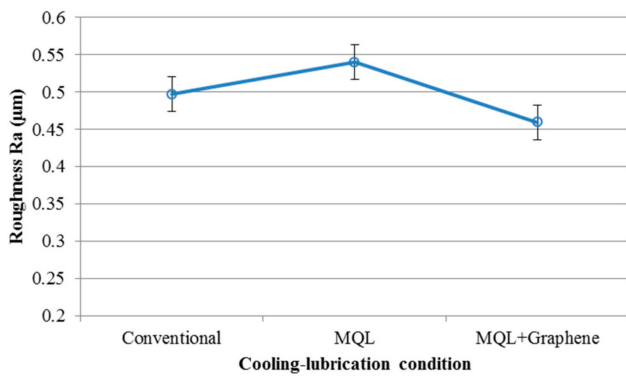
Roughness R_a	
Variable:	<i>p</i> -Value:
Radial depth of cut (a_e)	0.129180
Workspeed (V_w)	0.009680
Cooling-lubrication condition	0.693180
$a_e \times V_w$	0.337276
$a_e \times$ cooling-lubrication condition	0.488348
$V_w \times$ cooling-lubrication condition	0.862392
Roughness R_z	
Variable:	<i>p</i> -Value:
Radial depth of cut (a_e)	0.005487
Workspeed (V_w)	0.266157
Cooling-lubrication condition	0.534639
$a_e \times V_w$	0.953124
$a_e \times$ cooling-lubrication condition	0.085822
$V_w \times$ cooling-lubrication condition	0.996517



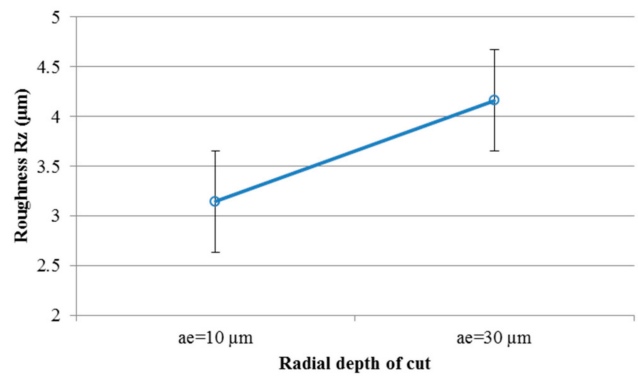
(a)



(b)



(c)



(d)

Figure 8. Cont.

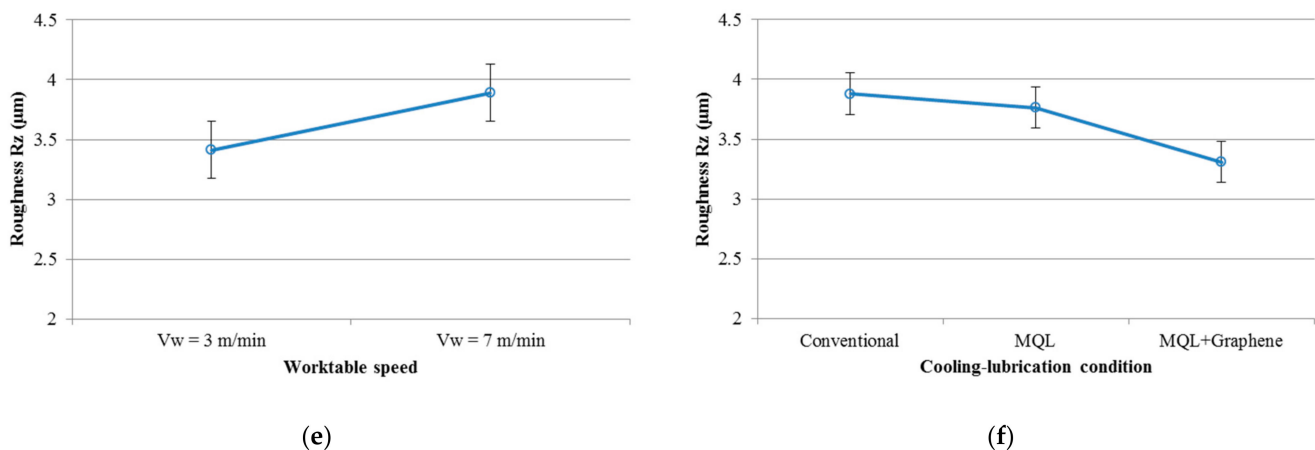


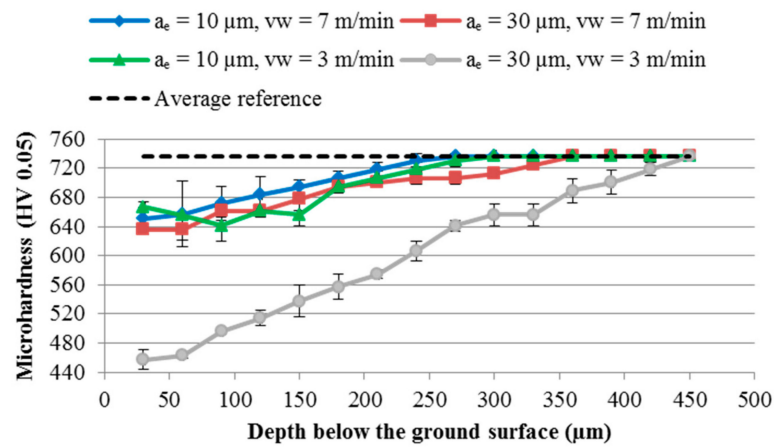
Figure 8. Effect of the input variables on the roughness parameter: (a) a_e in R_a ; (b) V_w in R_a ; (c) cooling–lubrication conditions in R_a ; (d) a_e in R_z ; (e) V_w in R_z ; (f) cooling–lubrication conditions in R_z .

3.2. Microhardness

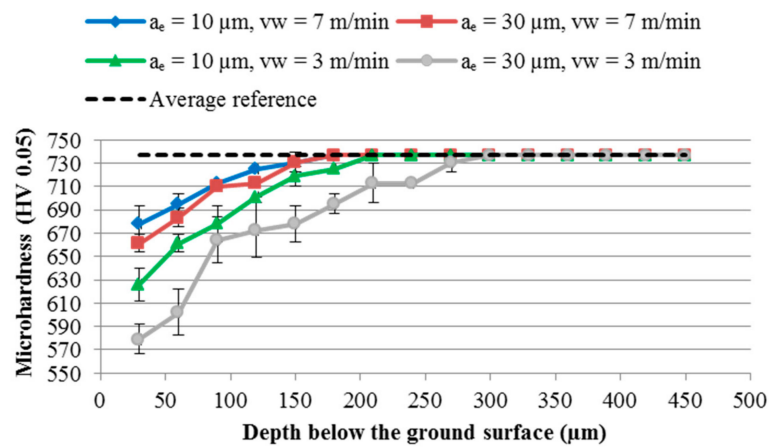
The plots of the Vickers microhardness profiles for grinding of SAE 52100 hardened steel with the three cooling–lubrication conditions are presented in Figure 9. The dashed line represents the microhardness value of the material before the grinding process (737 HV). Thus, each point in the graph corresponds to the average of three measurements taken in different regions, but at the same depth of the ground surface, for each workpiece.

According to the input variables for all the cooling–lubrication conditions employed, the behaviors of the microhardness values were similar. For all tests performed in the region close to the ground surface, there was a drop in microhardness in relation to the reference microhardness, and then the microhardness values increased with the distance from the machined surface. This behavior was probably due to the occurrence of excessive tempering, which was caused by the high temperatures developed in the process, causing the material in these regions to present a more ductile behavior, and thus presented a reduction in microhardness values [34]. Among all the input variables evaluated, the increase in parameter a_e was responsible for causing the most significant microhardness drops, as shown in Table 8, which presents the percentage drop in microhardness values in the region closest to the ground surface. When there is an increase in a_e , a more considerable amount of abrasive grits come into contact with the workpiece, thus increasing the area and the contact time, directly influencing the cutting region temperatures and, consequently, the chances of occurrence of thermal damage to the ground component [40]. Huang et al. [12] also observed this behavior in the peripheral surface grinding of NAK80 steel, and the increase of a_e resulted in the elevation of temperature values, consequently increasing the possibility of thermal damage. During the grinding of 20CrMnTi steel, Zhang et al. [41] observed a reduction in the hardness of the material with the increase of the radial depth of cut, and the authors explained that this behavior was due to the increase of the contact area grinding wheel/workpiece and, consequently, the number of particles acting in the cutting zone. As the value of a_e increases, the undeformed chip thickness per grit and the heat rate also increase, resulting in microstructural changes in the ground workpiece, reducing the material's hardness. The tests performed using the lowest workspeed (3 m/min) resulted in the most significant microhardness drops. For all cooling–lubrication conditions employed, the most significant drops were found in the tests using the most severe cutting conditions ($a_e = 30 \mu\text{m}$). In the tests using the radial depth of cut of $30 \mu\text{m}$, the most significant drop caused by the variation in the workspeed was found in the conventional cooling–lubrication condition, this drop being 28.1%. This behavior is explained by Rowe [1] as due to the time of contact between the grinding wheel and workpiece. The use of low workspeed (V_w) increases the possibility of thermal damage to the machined component since the process

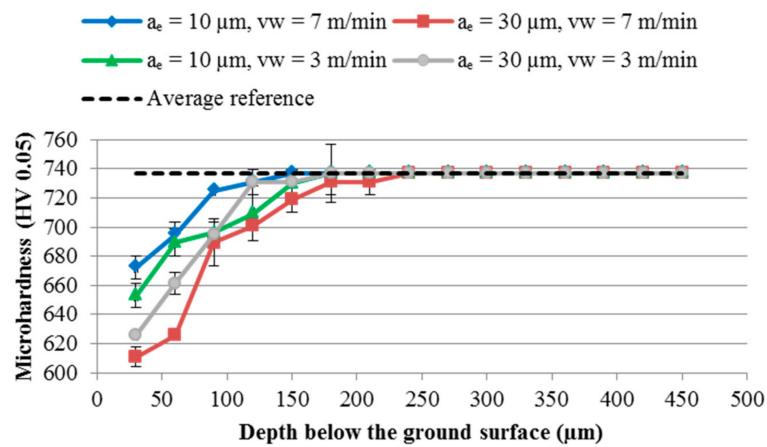
energy is concentrated in the contact region of the grinding wheel/workpiece for a more extended period.



(a)



(b)



(c)

Figure 9. Microhardness values below the surface for the SAE 52100 hardened steel obtained after peripheral surface grinding with aluminum oxide grinding wheel under different cooling–lubrication conditions: (a) conventional; (b) MQL; (c) MQL + Graphene.

Table 8. Percentage drop in microhardness values in a region close to the ground surface.

Cooling–Lubrication Condition	Workspeed (m/min)	Radial Depth of Cut (μm)	Percentage Drop in Relation to the Reference (%)
Conventional	3	10	9.50
		30	37.92
	7	10	11.60
		30	13.70
MQL	3	10	15.06
		30	21.44
	7	10	8.00
		30	10.24
MQL + Graphene	3	10	11.40
		30	15.06
	7	10	8.75
		30	17.10

In the tests performed using conventional and MQL cooling–lubrication conditions, it can be stated that the employ of $a_e = 30 \mu\text{m}$ and $V_w = 3 \text{ m/min}$ resulted in thermal damage to the ground component due to the high drop in microhardness values in comparison with the average microhardness of the material before the process. The cooling–lubrication conditions responsible for obtaining the smallest microhardness decreases were MQL + Graphene. The addition of solid particles to the cutting fluid contributed to improving the lubricant and thermal properties of the same (heat transfer), thus reducing the friction, cutting forces, and heat generated and diminishing thermal damage to the ground component [42]. In general, considering the more severe condition using $a_e = 30 \mu\text{m}$ and $V_w = 3 \text{ m/min}$, the use of graphene (MQL + Graphene) resulted in only a 15% reduction in the microhardness obtained after the grinding test, in the region closest to the ground surface, followed by the application of MQL without graphene, with 21%, and by the conventional condition, with 38%, as can be seen in Table 8. Furthermore, through the analysis of Figure 9, it can be stated that the thermal damages, represented by the microhardness variation, extended below the ground surface (the extent to which it was possible to observe the microhardness variation until reaching the average microhardness of the material) up to approximately $150 \mu\text{m}$ for the MQL + Graphene condition, $250 \mu\text{m}$ for the MQL condition, and $400 \mu\text{m}$ for the conventional condition. This result shows that graphene platelets to the cutting fluid positively influenced the process by minimizing thermal damage to the ground component under the investigated conditions. In other words, this behavior demonstrates the benefit of adding solid particles to the cutting fluid in terms of the sub-surface integrity of the ground components. The dispersion of the graphene platelets mainly contributes to the increase of the lubricating capacity of the fluid, thus reducing the generation of heat in the cutting zone and, consequently, the reduction of the area affected thermally by the portion of the heat that is directed to the workpiece. Consequently, some mechanical properties, such as hardness, are also less affected. As can be seen, compared to the MQL + Graphene condition, the MQL and conventional conditions showed an extension of thermal damage, respectively, 166.7% and 266.7% higher.

The p -values obtained by ANOVA for the microhardness are shown in Table 9. It was observed that with a 95% confidence interval, the radial depth of cut, workspeed, and the cooling–lubrication conditions, in addition to the interactions of a_e with V_w , and a_e and V_w with the cooling–lubrication condition, significantly influenced the results obtained. Figure 10 shows the behavior trends of the microhardness with changes in the cutting conditions. The increase of the radial depth of cut and the reduction of the workspeed resulted in lower values of the average microhardness. MQL + Graphene presented the average value closest to the material’s initial microhardness (737 HV). As shown in

Figure 10, the increase in radial depth of the cut from 10 μm to 30 μm provided a 3.6% reduction in the microhardness value, where this percentage was obtained by reducing the workspeed by 7 m/min; for 3 m/min, it was 3.29%. Regarding the cooling–lubrication conditions, the MQL and conventional conditions showed decreases in microhardness, respectively, equal to 0.7% and 5.98% in relation to the MQL + Graphene condition.

Table 9. Analysis of variance (ANOVA) for the microhardness values.

Variable	<i>p</i> -Value
Radial depth of cut (a_e)	0.000803
Workspeed (V_w)	0.002356
Cooling–lubrication condition	0.0000255
$a_e \times V_w$	0.038352
$a_e \times$ cooling–lubrication condition	0.004386
$V_w \times$ cooling–lubrication condition	0.007282

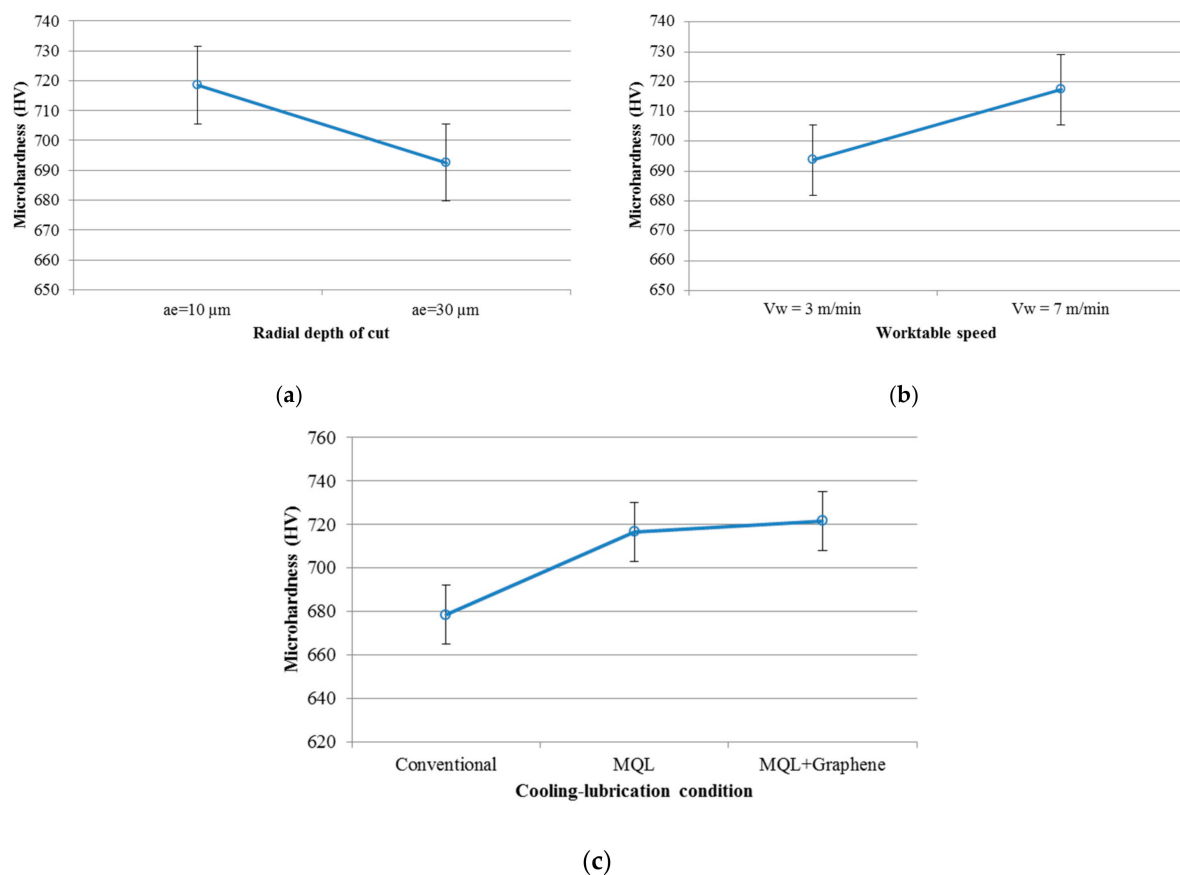


Figure 10. Effect of the input variables on the microhardness: (a) a_e ; (b) V_w ; (c) cooling–lubrication conditions.

3.3. Images of the Ground Surfaces

The scanning electron microscope (SEM) images of the SAE 52100 hardened steel ground surfaces under different cutting and cooling–lubrication conditions are shown in Figure 11. The ground surfaces presented a similar pattern, with grooves mainly oriented in the cutting direction and regions containing flaws and material side flow, followed by adhered material. Usually, grooves oriented in the cutting direction are preferable, as this indicates that the grits have been active and removed the material from the workpiece. Nevertheless, the flaws, material side flow, and adhered material represent surface defects.

These events usually occur due to the deficiency of the cooling–lubrication conditions in cooling and/or lubricating the system. In other words, the surfaces that present the most significant amount of these defects result from tests performed with unfavorable tribological conditions [31,43]. Majumdar et al. [44] also point out that processes with better cooling and lubricating properties keep the abrasive grits sharpened for longer, resulting in a machined surface with a better surface texture with fewer defects.

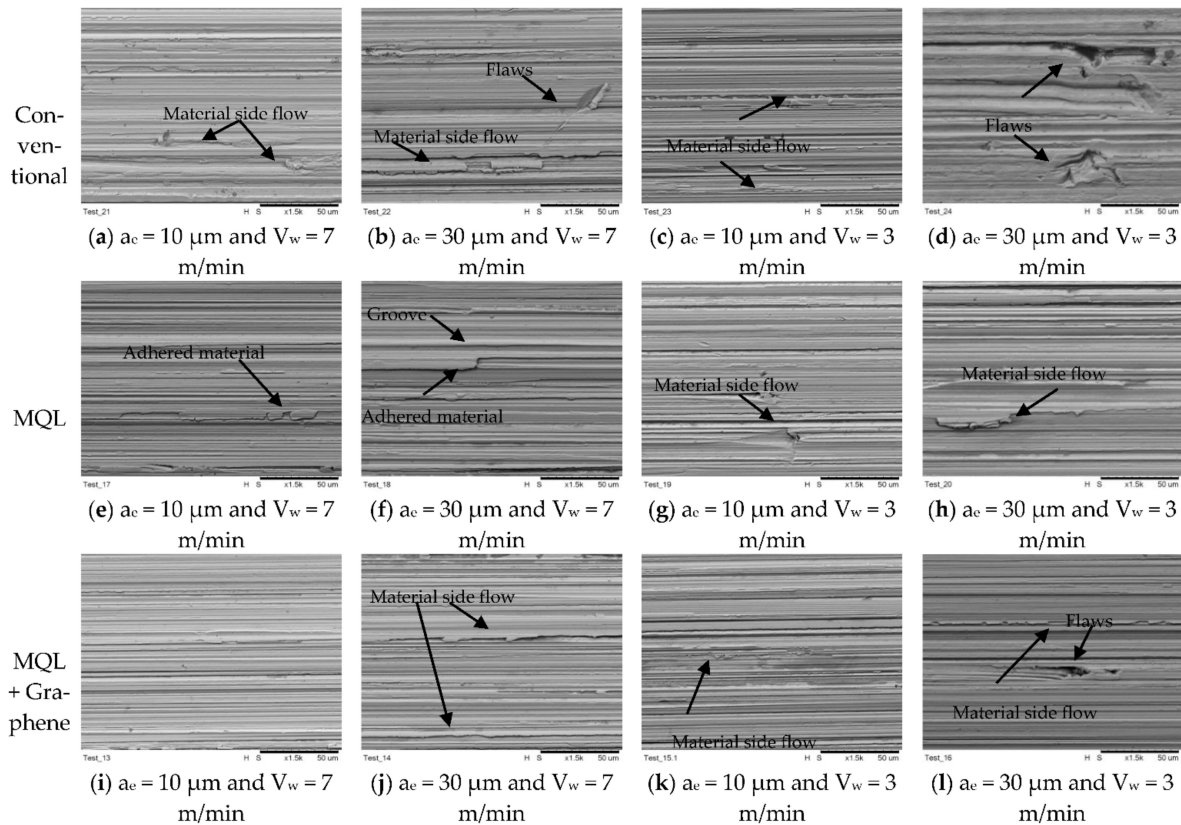


Figure 11. SEM images of the ground surfaces obtained employing different cutting and cooling–lubrication conditions.

In the more severe cutting conditions ($a_e = 30 \mu\text{m}$), a more significant number of areas with flaws, material side flow, and grooves were found that were not so uniform, with a greater thickness and depth than the tests carried out using $a_e = 10 \mu\text{m}$. This behavior was also observed in a study developed by Li et al. [45], who reported the presence of only elastic and plastic deformations after machining at the lowest values of a_e , while the more significant number of areas with plastic deformations and consequently material side flow, in regions with material chipping (flaws), that adversely affect surface finishing were observed after machining with the highest values of a_e . In general, the workspeed variation did not significantly change the results regarding the quality of the ground components' surface textures. Nevertheless, it was possible to observe that the surfaces obtained after the tests carried out using the workspeed of 3 m/min showed a more significant amount of material side flow and flaws compared to the surfaces originating from the tests using $V_w = 7$ m/min, especially in more severe cutting conditions ($a_e = 30 \mu\text{m}$). According to Rowe [1], the use of low workspeed values results in a longer contact time between the grinding wheel and the workpiece, making the energy generated in the process become concentrated in the cutting zone for a longer time and, therefore, being unfavorable with respect to the finish of the machined components. No cracks were found in any sample of SAE 52100 steel under the cooling–lubrication conditions investigated.

Among all the evaluated cooling–lubrication conditions, the use of the cutting fluid containing dispersed multilayer graphene platelets was responsible for the better finishing surfaces, while the surfaces obtained through the conventional condition were the worst.

The surfaces obtained after grinding using the MQL + Graphene cooling–lubrication conditions showed less plastic deformation and material side flow, as well as and adhered material, and practically no flaws, and the grooves generated showed greater uniformity and less depth. The addition of graphene platelets improves cutting fluid properties, such as increased viscosity and solid lubricants at the grinding wheel/workpiece interface. Thus, there is greater lubrication of the system, reducing the friction generated during machining and facilitating the cutting of the material, contributing to the generation of components with better surface texture [46]. Although solid particles also significantly increase fluid viscosity, this cutting fluid was used in the grinding process through the MQL cooling–lubrication condition. In this condition, tiny fluid droplets are propelled employing compressed air (0.3 MPa) to the cutting zone. Thus, nozzle blocking due to graphene platelets is practically unlikely for this condition. Furthermore, it was observed that the significant increase in viscosity provided better lubrication of the contact region between the grinding wheel and the workpiece, resulting in surfaces with a better surface finish. Huang et al. [12] observed the positive influence of the addition of MWCNT (multi-walled carbon nanotube) platelets to the cutting fluid on NAK80 steel ground surfaces compared to dry and MQL tests applying pure fluid, which they attributed to the formation of a thin film, under high pressure and temperature, on the surface, improving the lubrication of the cutting region and, thus, producing machined surfaces with better quality. The dispersion of solid particles to the cutting fluid also improved the surface texture of AISI 52100 hardened steel submitted to the grinding process in a study developed by Mao et al. [39].

In the analysis by scanning electron microscopy (SEM) and an energy dispersive system (EDS) aid, graphene platelets were found on all ground surfaces using the MQL + Graphene cooling–lubrication conditions, regardless of the cutting conditions employed, as observed in Figure 12. The surface shown in Figure 12 refers to tests performed using cutting conditions $a_e = 10 \mu\text{m}$ and $V_w = 7 \text{ m/min}$. This result is beneficial because these particles can act as solid lubricants, thus reducing the friction during the use of these components and facilitating the heat exchange between the piece and the environment due to the good thermal properties of graphene.

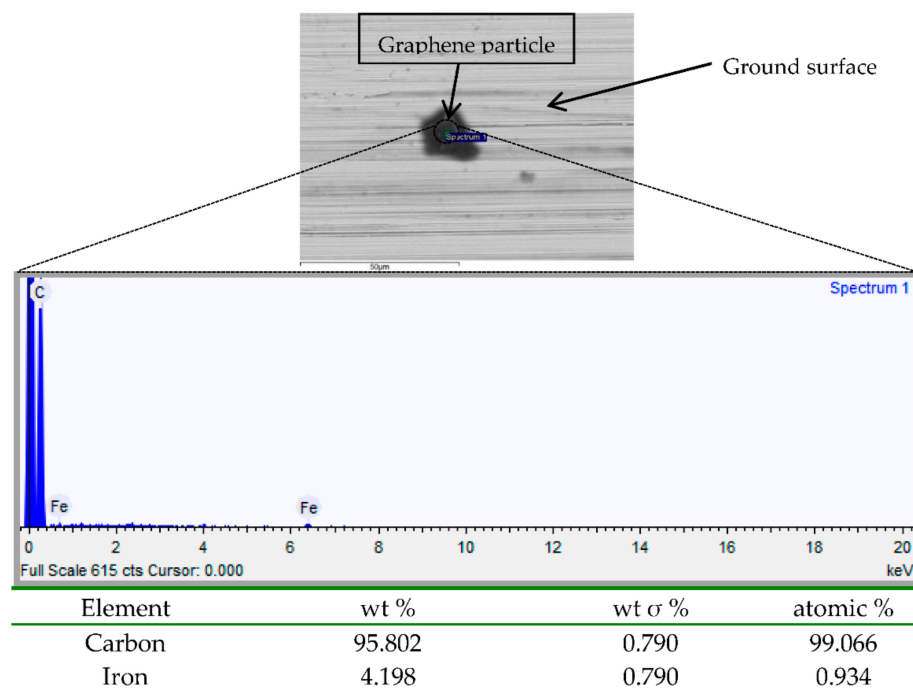


Figure 12. Results of the analysis (EDS) of material on the workpiece’s surface evidencing the presence of graphene platelets after the grinding.

4. Conclusions

According to the experimental results obtained with peripheral surface grinding of SAE 52100 hardened steel under different cutting and cooling–lubrication conditions, the following conclusions can be drawn:

- The R_a parameter recorded for SAE 52100 steel grade stayed below $0.63\ \mu\text{m}$, which is considered the upper limit for semi-finishing grinding. Roughness parameters R_a and R_z increased with the radial depth of cut (a_e) and the workspeed (V_w);
- Presence of graphene generated surfaces with lower roughness values than conventional that, in general, present larger values;
- With respect to the microhardness values, it was observed that the conventional condition generated the highest drop (38%) in relation to the initial microhardness of the material (before grinding process), and under certain conditions, these falls, due to the magnitude, represented the presence of thermal damage to the component;
- The use of the MQL + Graphene generated the lowest variation of microhardness values (15%). The increase of a_e and the reduction of V_w resulted in the most significant drop with respect to the initial microhardness of the material (before the grinding process);
- As the radial depth of cut increased, areas with plastic deformation, material side flow, flaws, and adhered material also increased. Regarding the cooling–lubrication conditions, it was possible to observe that the surfaces with better surface texture were obtained after grinding tests using the MQL + Graphene condition;
- In order to evaluate the influence of the cooling–lubrication conditions based on the parameters' roughness, microhardness, and analysis of surface machined, the order of performance of these conditions in relation to the cutting parameters employed was 1st MQL + Graphene, 2nd MQL, and 3rd Conventional.

Author Contributions: Conceptualization, B.S.A. and R.B.d.S.; methodology, B.S.A. and R.B.d.S.; validation, B.S.A. and M.F.P.; formal analysis, B.S.A.; investigation, B.S.A.; resources, R.B.d.S., R.V.G. and F.M.C.d.F.; writing—original draft preparation, B.S.A.; writing—review and editing, B.S.A., R.B.d.S., M.F.P., L.R.R.d.S., A.R.M. and M.M. All authors have read and agreed to the published version of the manuscript.

Funding: This study was financed in part by the Coordenação de Aperfeiçoamento de Pessoal de Nível Superior—Brasil (CAPES)—Finance Code 001. The authors are grateful to the FAPEMIG and the Post Graduate Program of Mechanical Engineering of UFU for financial support. In addition, one of the authors thanks FAPEMIG and CNPq for the financial support received through the PPM-XII Project, Process No. PPM 00492-18, and Process No. 426018/2018-4.

Acknowledgments: The authors are grateful to Saint Gobain Abrasives and Blaser Swisslube Brasil for supporting this work with the donation of grinding wheels and cutting fluid, respectively.

Conflicts of Interest: The authors declare no conflict of interest.

References

1. Rowe, W.B. *Principles of Modern Grinding Technology*, 2nd ed.; Elsevier Inc.: Amsterdam, The Netherlands, 2014.
2. Klocke, F. *Manufacturing Processes 2: Grinding, Honing and Lapping*, 1st ed.; Springer: Berlin/Heidelberg, Germany, 2009.
3. Alves, J.A.C.; Fernandes, U.D.B.; Júnior, C.E.D.S.; Bianchi, E.C.; De Aguiar, P.R.; Da Silva, E.J. Application of the Minimum Quantity Lubrication (MQL) technique in the plunge cylindrical grinding operation. *J. Braz. Soc. Mech. Sci. Eng.* **2009**, *31*, 1–4. [[CrossRef](#)]
4. Gupta, M.K.; Song, Q.; Liu, Z.; Sarikaya, M.; Jamil, M.; Mia, M.; Singla, A.K.; Khan, A.M.; Khanna, N.; Pimenov, D.Y. Environment and economic burden of sustainable cooling/lubrication methods in machining of Inconel-800. *J. Clean. Prod.* **2021**, *287*, 125074. [[CrossRef](#)]
5. Sanchez, J.A.; Pombo, I.; Alberdi, R.; Izquierdo, B.; Ortega, N.; Plaza, S.; Martinez-Toledano, J. Machining evaluation of a hybrid MQL-CO₂ grinding technology. *J. Clean. Prod.* **2010**, *18*, 1840–1849. [[CrossRef](#)]
6. Walker, T. *The MQL Handbook—A Guide to Machining with Minimum Quantity Lubrication*; Unist Inc.: Grand Rapids, MI, USA, 2013.
7. Hadad, M.; Tawakoli, T.; Sadeghi, M.; Sadeghi, B. Temperature and energy partition in minimum quantity lubrication-MQL grinding process. *Int. J. Mach. Tools Manuf.* **2012**, *54–55*, 10–17. [[CrossRef](#)]

8. Bianchi, E.C.; Rodriguez, R.L.; Hildebrandt, R.A.; Lopes, J.C.; De Mello, H.J.; Da Silva, R.B.; De Aguiar, P.R. Plunge cylindrical grinding with the minimum quantity lubrication coolant technique assisted with wheel cleaning system. *Int. J. Adv. Manuf. Technol.* **2017**, *95*, 2907–2916. [[CrossRef](#)]
9. Hadad, M.; Sadeghi, B. Thermal analysis of minimum quantity lubrication-MQL grinding process. *Int. J. Mach. Tools Manuf.* **2012**, *63*, 1–15. [[CrossRef](#)]
10. Hadad, M.; Sharbati, A. Thermal Aspects of Environmentally Friendly-MQL Grinding Process. *Procedia CIRP* **2016**, *40*, 509–515. [[CrossRef](#)]
11. Wang, Y.; Li, C.; Zhang, Y.; Li, B.; Yang, M.; Zhang, X.; Guo, S.; Liu, G.; Zhai, M. Comparative evaluation of the lubricating properties of vegetable-oil-based nanofluids between frictional test and grinding experiment. *J. Manuf. Process.* **2017**, *26*, 94–104. [[CrossRef](#)]
12. Huang, W.T.; Liu, W.S.; Wu, D.H. Investigations into lubrication in grinding processes using MWCNTs nanofluids with ultrasonic-assisted dispersion. *J. Clean. Prod.* **2016**, *137*, 1553–1559. [[CrossRef](#)]
13. Zhang, Y.; Li, C.; Yang, M.; Jia, D.; Wang, Y.; Li, B.; Hou, Y.; Zhang, N.; Wu, Q. Experimental evaluation of cooling performance by friction coefficient and specific friction energy in nanofluid minimum quantity lubrication grinding with different types of vegetable oil. *J. Clean. Prod.* **2016**, *139*, 685–705. [[CrossRef](#)]
14. Wojtewicz, M.; Nadolny, K.; Kapłonek, W.; Rokosz, K.; Matýsek, D.; Ungureanu, M. Experimental studies using minimum quantity cooling (MQC) with molybdenum disulfide and graphite-based microfluids in grinding of Inconel[®] alloy 718. *Int. J. Adv. Manuf. Technol.* **2018**, *101*, 637–661. [[CrossRef](#)]
15. Silva, R.B.; Ezugwu, E.O.; Guimarães, C.; Marques, A.; Fernandes, L.A.; Gelamo, R.V. Grinding of mould steel with graphene platelets dispersed in a vegetable-based cutting fluids. In Proceedings of the STLE Annual Meeting & Exhibition, Dallas, TX, USA, 15–21 May 2015.
16. Chu, B.; Singh, E.; Koratkar, N.; Samuel, J. Graphene-Enhanced Environmentally-Benign Cutting Fluids for High-Performance Micro-Machining Applications. *J. Nanosci. Nanotechnol.* **2013**, *13*, 5500–5504. [[CrossRef](#)] [[PubMed](#)]
17. Pavan, R.B.; Gopal, A.V.; Amrita, M.; Goriparthi, B.K. Experimental investigation of graphene nanoplatelets-based minimum quantity lubrication in grinding Inconel 718. *Proc. Inst. Mech. Eng. Part B J. Eng. Manuf.* **2019**, *233*, 400–410. [[CrossRef](#)]
18. De Oliveira, D.; Da Silva, R.; Gelamo, R. Influence of multilayer graphene platelet concentration dispersed in semi-synthetic oil on the grinding performance of Inconel 718 alloy under various machining conditions. *Wear* **2019**, *426–427*, 1371–1383. [[CrossRef](#)]
19. Li, M.; Yu, T.; Zhang, R.; Yang, L.; Ma, Z.; Li, B.; Wang, X.; Wang, W.; Zhao, J. Experimental evaluation of an eco-friendly grinding process combining minimum quantity lubrication and graphene-enhanced plant-oil-based cutting fluid. *J. Clean. Prod.* **2020**, *244*, 118747. [[CrossRef](#)]
20. Ibrahim, A.M.M.; Li, W.; Xiao, H.; Zeng, Z.; Ren, Y.; Alsoofi, M.S. Energy conservation and environmental sustainability during grinding operation of Ti-6Al-4V alloys via eco-friendly oil/graphene nano additive and Minimum quantity lubrication. *Tribol. Int.* **2020**, *150*, 106387. [[CrossRef](#)]
21. De Paiva, R.L.; Ruzzi, R.D.S.; De Oliveira, L.R.; Filho, E.P.B.; Neto, L.M.G.; Gelamo, R.V.; Da Silva, R.B. Experimental study of the influence of graphene platelets on the performance of grinding of SAE 52100 steel. *Int. J. Adv. Manuf. Technol.* **2020**, *110*, 1–12. [[CrossRef](#)]
22. Guimarães, C.; Da Silva, R.B.; Ruzzi, R.D.S.; De Mello, A.V.; Hübner, H.B.; Fiocchi, A.A.; Fonseca, M.C. Evaluation of surface and sub-surface integrities of a mold steel under different grinding conditions. *J. Braz. Soc. Mech. Sci. Eng.* **2019**, *41*, 435. [[CrossRef](#)]
23. Hübner, H.B.; Da Silva, R.B.; Duarte, M.A.V.; Da Silva, M.; Ferreira, F.I.; De Aguiar, P.R.; Baptista, F.G. A comparative study of two indirect methods to monitor surface integrity of ground components. *Struct. Health Monit.* **2020**, *19*, 1856–1870. [[CrossRef](#)]
24. Abrão, B.S.; Pereira, M.F.; Guimarães, C.; Da Silva, L.S.V.; Ruzzi, R.D.S.; Da Silva, R.B.; Bianchi, E.C.; Machado, A.R. Surface Finish Evaluation of AISI P100 Steel after Grinding with MQL Technique with Different Flow Rates. *J. Mech. Eng. Autom.* **2020**, *10*, 60–65. [[CrossRef](#)]
25. Rouxinol, F.P.; Gelamo, R.V.; Amici, R.G.; Vaz, A.R.; Moshkalev, S.A. Low contact resistivity and strain in suspended multilayer graphene. *Appl. Phys. Lett.* **2010**, *97*, 253104. [[CrossRef](#)]
26. Wong, H.-S.P.; Akinwande, D. *Carbon Nanotube and Graphene Device Physics*; Cambridge University Press: Cambridge, UK, 2009.
27. De Mello, A.; de Silva, R.B.; Machado, A.V.; Gelamo, R.V.; Diniz, A.E.; de Oliveira, R.F.M. Surface Grinding of Ti-6Al-4V Alloy with SiC Abrasive Wheel at Various Cutting Conditions. *Procedia Manuf.* **2017**, *10*, 590–600. [[CrossRef](#)]
28. Da Silva, R.B.; Lima, M.L.S.; Pereira, M.F.; Abrão, B.S.; da Silva, L.R.R.; Bianchi, E.C.; Machado, A.R. A surface and sub-surface quality evaluation of three cast iron grades after grinding under various cutting conditions. *Int. J. Adv. Manuf. Technol.* **2018**, *99*, 1839–1852. [[CrossRef](#)]
29. De Moraes, D.L.; Garcia, M.V.; Lopes, J.C.; Ribeiro, F.S.F.; Sanchez, L.E.D.A.; Foschini, C.R.; de Mello, H.J.; Aguiar, P.R.; Bianchi, E.C. Performance of SAE 52100 steel grinding using MQL technique with pure and diluted oil. *Int. J. Adv. Manuf. Technol.* **2019**, *105*, 4211–4223. [[CrossRef](#)]
30. Srivastava, A.; Awale, A.; Vashista, M.; Yusufzai, M.Z.K. Monitoring of thermal damages upon grinding of hardened steel using Barkhausen noise analysis. *J. Mech. Sci. Technol.* **2020**, *34*, 2145–2151. [[CrossRef](#)]
31. Javaroni, R.L.; Lopes, J.C.; Garcia, M.V.; Ribeiro, F.S.F.; Sanchez, L.E.D.A.; De Mello, H.J.; Aguiar, P.R.; Bianchi, E.C. Grinding hardened steel using MQL associated with cleaning system and cBN wheel. *Int. J. Adv. Manuf. Technol.* **2020**, *107*, 2065–2080. [[CrossRef](#)]

32. Garcia, M.V.; Lopes, J.C.; Diniz, A.E.; Rodrigues, A.R.; Volpato, R.S.; Sanchez, L.; de Mello, H.J.; Aguiar, P.R.; Bianchi, E.C. Grinding performance of bearing steel using MQL under different dilutions and wheel cleaning for green manufacture. *J. Clean. Prod.* **2020**, *257*, 120376. [[CrossRef](#)]
33. *Especificações Geométricas do Produto (GPS)-Rugosidade: Método do Perfil-Termos, Definições e Parâmetros da Rugosidade*; ABNT NBR ISO 4287; ABNT—Associação Brasileira de Normas Técnica: Rio de Janeiro, Brazil, 2002. (In Portuguese)
34. Malkin, S.; Guo, C. *Grinding Technology: Theory and Applications of Machining with Abrasives*, 2nd ed.; Industrial Press: New York, NY, USA, 2008.
35. Lin, B.; Zhou, P.; Wang, Z.; Yan, Y.; Kang, R.; Guo, D. Analytical Elastic–Plastic Cutting Model for Predicting Grain Depth-of-Cut in Ultrafine Grinding of Silicon Wafer. *J. Manuf. Sci. Eng.* **2018**, *140*, 121001. [[CrossRef](#)]
36. Tawakoli, T.; Hadad, M.; Sadeghi, M.; Daneshi, A.; Stöckert, S.; Rasifard, A. An experimental investigation of the effects of workpiece and grinding parameters on minimum quantity lubrication—MQL grinding. *Int. J. Mach. Tools Manuf.* **2009**, *49*, 924–932. [[CrossRef](#)]
37. Sadeghi, M.H.; Hadad, M.J.; Tawakoli, T.; Vesali, A.; Emami, M. An investigation on surface grinding of AISI 4140 hardened steel using minimum quantity lubrication-MQL technique. *Int. J. Mater. Form.* **2010**, *3*, 241–251. [[CrossRef](#)]
38. Gao, T.; Li, C.; Zhang, Y.; Yang, M.; Jia, D.; Jin, T.; Hou, Y.; Li, R. Dispersing mechanism and tribological performance of vegetable oil-based CNT nanofluids with different surfactants. *Tribol. Int.* **2019**, *131*, 51–63. [[CrossRef](#)]
39. Mao, C.; Tang, X.; Zou, H.; Huang, X.; Zhou, Z. Investigation of grinding characteristic using nanofluid minimum quantity lubrication. *Int. J. Precis. Eng. Manuf.* **2012**, *13*, 1745–1752. [[CrossRef](#)]
40. Morris, T. *Abrasive Machining with MQL*. Ph.D. Thesis, Cranfield University, Cranfield, UK, 2011.
41. Zhang, Y.; Li, B.; Yang, J.; Liang, S. Modeling and optimization of alloy steel 20CrMnTi grinding process parameters based on experiment investigation. *Int. J. Adv. Manuf. Technol.* **2017**, *95*, 1859–1873. [[CrossRef](#)]
42. Li, B.; Li, C.; Zhang, Y.; Wang, Y.; Yang, M.; Jia, D.; Zhang, N.; Wu, Q.; Ding, W. Numerical and experimental research on the grinding temperature of minimum quantity lubrication cooling of different workpiece materials using vegetable oil-based nanofluids. *Int. J. Adv. Manuf. Technol.* **2017**, *93*, 1971–1988. [[CrossRef](#)]
43. Ruzzi, R.D.S.; da Silva, L.R.R.; da Silva, R.B.; da Silva, W.M., Jr.; Bianchi, E.C. Topographical analysis of machined surfaces after grinding with different cooling-lubrication techniques. *Tribol. Int.* **2020**, *141*, 105962. [[CrossRef](#)]
44. Majumdar, S.; Das, P.; Kumar, S.; Roy, D.; Chakraborty, S. Evaluation of cutting fluid application in surface grinding. *Measurement* **2021**, *169*, 108464. [[CrossRef](#)]
45. Li, H.; Yu, T.B.; Da Zhu, L.; Wang, W.S. Analytical modeling of ground surface topography in monocrystalline silicon grinding considering the ductile-regime effect. *Arch. Civ. Mech. Eng.* **2017**, *17*, 880–893. [[CrossRef](#)]
46. Chakule, R.R.; Chaudhari, S.S.; Talmale, P.S. Optimization of Nanofluid Minimum Quantity Lubrication (NanoMQL) Technique for Grinding Performance Using Jaya Algorithm. *Adv. Intell. Syst. Comput.* **2019**, *969*, 211–221. [[CrossRef](#)]